# Synthesis of Extremely Small CdSe and Bright Blue Luminescent CdSe/ZnS Nanoparticles by a Prefocused Hot-Injection Approach

Richard Karel Čapek,*,† Karel Lambert,† Dirk Dorfs,‡ Philippe Frederic Smet,§ Dirk Poelman,§ Alexander Eychmüller,|| and Zeger Hens†,⊥

*Physics and Chemistry of Nanostructures, Ghent University, Krijgslaan 281-S12, 9000 Ghent, Belgium, Istituto Italiano di Tecnologia, via Morego 30, 16163 Genoa, Italy, Lumilab, Department of Solid State Sciences, Ghent University, Krijgslaan 281-S1, 9000 Ghent, Belgium, and Physical Chemistry and Electrochemistry, Technical University Dresden, Bergstrasse 66b, 01062 Dresden, Germany*

*Received January 27, 2009*

Although cadmium selenide is a well-explored material in aqueous and hot-injection synthesis of semiconductor quantum dots, only a few syntheses are reported for the preparation of extremely small cadmium selenide nanocrystallites. We present a hot-injection approach based on the enhancement of the nucleation rate to make cadmium selenide quantum dots with a diameter tunable between 1.5 and 2.2 nm. Furthermore, we present a procedure on how to coat these particles with zinc sulfide, leading to highly efficient fluorophors in the blue region of the visible spectrum. The work was performed without the use of highly reactive (pyrophoric) precursors and represents a basic concept for the preparation of small nanoparticles in general.

## Introduction

Colloidal semiconductor nanoparticles or quantum dots (QDs) are a relatively young class of fluorescent dyes. Because of their unique properties, e.g., the tunability of the emission wavelength due to the size quantization effect, they are interesting materials to be used in different applications like, e.g., biolabeling, light-emitting diodes (LEDs), solar cells, and lasers.[1−6] The exploration of these different applications has been driven by the development of reproducible synthesis schemes that yield highly monodisperse colloidal quantum dot dispersions. Especially in the case of cadmium selenide (CdSe), the hot-injection approach[7] has resulted in sizable syntheses that use less hazardous chemicals and yield highly monodisperse batches of QDs with a QD size depending on the reaction time.[8−10] Therefore, CdSe QDs have become a standard material of research on colloidal nanomaterials today.

The use of QDs as light emitters requires an emission that is stable against photo and chemical degradation, and that features a high photoluminescence quantum yield. These demands can be met by coating the QD surface with inorganic materials which have a broader band gap that encompasses the band gap of the core QD (type 1 band alignment). This was demonstrated, among others, in the case of CdSe/ZnS and CdS/ZnS core/shell nanoparticles.[11−13] The longest peak emission wavelength reported for CdS/ZnS nanoparticles is about 480 nm and the shortest peak emission wavelengths reported for CdSe/ZnS by hot injection and for cluster-based approaches are 470 and 460 nm,[12] respectively. This means that cadmium chalcogenide type-I core−shell particles bear the potential to be used as fluorophores covering a gapless range from the UV to the deep red region of the visible spectrum. Until now, freely sizable syntheses of CdSe QDs in a size range below 2 nm were demonstrated only in the aqueous phase and in a two-phase autoclave system.[14,15] A sizable hot-injection synthesis has not been developed yet. Hot-injection procedures for CdSe/ZnS core−shell QDs with emission wavelengths below 500 nm reported so far typically use fractions of small nanoparticles which are isolated by size selective precipitation from a

* To whom correspondence should be addressed. E-mail: richard.capek@ugent.be. Tel.: 0032 9 264 48 74. Fax: 0032 9 264 49 83.
† Physics and Chemistry of Nanostructures, Ghent University.
‡ Istituto Italiano di Tecnologia.
§ Lumilab, Department of Solid State Sciences, Ghent University.
|| Technical University Dresden.
⊥ E-mail: zeger.hens@ugent.be

(1) Mattoussi, H.; Mauro, J. M.; Goldman, E. R.; Anderson, G. P.; Sundar, V. C.; Mikulec, F. V.; Bawendi, M. G. *J. Am. Chem. Soc.* **2000**, *122*, 12142.
(2) Coe-Sullivan, S.; Woo, W. K.; Steckel, J. S.; Bawendi, M.; Bulovic, V. *Org. Electron.* **2003**, *4*, 123.
(3) Vogel, R.; Pohl, K.; Weller, H. *Chem. Phys. Lett.* **1990**, *174*, 241.
(4) Vogel, R.; Hoyer, P.; Weller, H. *J. Phys. Chem.* **1994**, *98*, 3183.
(5) Huynh, W. U.; Dittmer, J. J.; Alivisatos, A. P. *Science* **2002**, *295*, 2425.
(6) Htoon, H.; Hollingworth, J. A.; Malko, A. V.; Dickerson, R.; Klimov, V. I. *Appl. Phys. Lett.* **2003**, *82*, 4776.
(7) Murray, C. B.; Norris, D. J.; Bawendi, M. G. *J. Am. Chem. Soc.* **1993**, *115*, 8706.
(8) Peng, Z. A.; Peng, X. G. *J. Am. Chem. Soc.* **2002**, *124*, 3343.
(9) Mekis, I.; Talapin, D. V.; Kornowski, A.; Haase, M.; Weller, H. *J. Phys. Chem. B* **2003**, *107*, 7454.
(10) Jasieniak, J.; Bullen, C.; van Embden, J.; Mulvaney, P. *J. Phys. Chem. B* **2005**, *109*, 20665.
(11) Hines, M. A.; Guyot-Sionnest, P. *J. Phys. Chem.* **1996**, *100*, 468.
(12) Dabbousi, B. O.; RodriguezViejo, J.; Mikulec, F. V.; Heine, J. R.; Mattoussi, H.; Ober, R.; Jensen, K. F.; Bawendi, M. G. *J. Phys. Chem. B* **1997**, *101*, 9463.
(13) Steckel, J. S.; Zimmer, J. P.; Coe-Sullivan, S.; Stott, N. E.; Bulovic, V.; Bawendi, M. G. *Angew. Chem.-Int. Ed.* **2004**, *43*, 2154.
(14) Pan, D. C.; Wang, Q.; Jiang, S. C.; Ji, X. L.; An, L. J. *Adv. Mater.* **2005**, *17*, 176.
(15) Rogach, A. L.; Kornowski, A.; Gao, M. Y.; Eychmuller, A.; Weller, H. *J. Phys. Chem. B* **1999**, *103*, 3065.

10.1021/cm900248b CCC: $40.75 
Published on Web 03/18/2009

reaction product with broad size distributions.[7,16] These pathways are unfavorable due to the synthetic effort and the consumption of chemicals they require. Recently, also the synthesis of magic-sized nanoparticles has been demonstrated where specific cluster sizes could be prepared without the presence of others, but these were not used for core−shell QDs.[17]

Here, we present a hot-injection-based synthesis that is designed to gain colloids of highly monodisperse CdSe QDs with diameters tunable between 2.2 and 1.6 nm, size dispersion in diameter below 5%, and a reaction yield sufficient for further processing. This result is achieved by the adjustment of the reaction conditions toward a small critical radius and a high nucleation rate based on theoretical assumptions.[18,19] Furthermore, we show that the resulting CdSe QDs can be coated with ZnS to produce efficient emitters in the blue region of the visible spectrum. So far, hot-injection procedures represent the most widespread and successful pathway for the synthesis of high-quality colloidal QDs of a large number of different materials. Therefore, a hot-injection-based approach for extremely small QDs of a certain material as exemplified here for CdSe might represent a general pathway for the synthesis of other materials.

## Experimental Section

**Chemicals.** Oleylamine (OLA; 80−90%) was purchased from Acros, chloroform, toluene, methanol and 2-propanol were purchased from VWR BDH Prolabo, and all were Rectapur grade. Hexane and heptane were also purchased from BDH Prolabo and were Normapur grade. Hexadecylamine (HDA) and stearic acid were purchased from Merck and were synthesis grade. Oleic acid and 2-octadecene (ODE) were purchased from Aldrich and were technical grade (90%). Zinc acetate (99.99%) and cadmium oxide (CdO; 99.99+%) were also purchased from Aldrich. Selenium (99.999%) was purchased from Alfa Aesar. Trioctylphospine (TOP, 97%) and sulfur (99.999%) were purchased from Strem. Cadmium carboxylate mixtures (cadmium to acid ratio = 1:3) were prepared by mixing CdO and the particular acid in a 1:3 molar ratio, degassing for 1 h at 100 °C under a nitrogen flow, and dissolving the cadmium oxide under a nitrogen atmosphere at about 250 °C.

**Typical Core Synthesis.** Cadmium carboxylate (0.2 mmol; calculated on cadmium), 0.6 mmol of HDA, and 10 mL of ODE were degassed for 1 h at room temperature and 1 h at 100 °C under a nitrogen flow in a 25 mL four-necked flask. Under a nitrogen atmosphere (nitrogen flow in the case of a reaction stop with low boiling solvents) the temperature was raised to the injection temperature and 2 mL of a 1 M TOPSe solution (2 mmol of selenium dissolved in 2 mL of TOP) were injected.

In the case of reaction monitoring, stearic acid was used as carboxylic acid. The injection temperature was set to 245 °C and the growth temperature was adjusted at 230 °C. Aliquots were taken after certain times and directly dissolved in chloroform. Absorption spectra of these aliquots were recorded with no further treatment.

In the case of a reaction stop after 5 s, oleic acid was used as carboxylic acid. The injection temperature was varied between 230 and 170 °C. The reaction was stopped by the injection of 10 mL of a solvent at 20 °C. In the case of a synthesis of bigger particles (about 3 nm in diameter) stearic acid was used as carboxylic acid. The injection temperature was 245 °C and the growth temperature 230 °C.

After the reactions were performed, typically about 10 mL of toluene was added to the raw material and the nanoparticles were precipitated by adding a 1:1−1:2 mixture of 2-propanol and methanol. The precipitate was separated by centrifugation and redissolved in hexane.

**Typical Coating Procedure.** Under a nitrogen atmosphere, the zinc precursor solution (0.04 M zinc acetate and 0.32 M OLA in ODE) and 0.04 M ODES (sulfur dissolved in ODE) were mixed with ODE to reach a total volume of 4 mL. The amounts of the precursors added were calculated to obtain a shell thickness of two monolayers according to the literature.[20,21] Then a solution of $10^{-4}$ mmol nanoparticles in hexane was injected. The reaction mixture was heated up to 100 °C and maintained for 3 h at this temperature (time was taken from the moment when the reaction mixture reached a temperature of 90 °C). Then the reaction mixture was cooled down to room temperature. Under ambient conditions, 4 mL of toluene and 400 $\mu$L of oleic acid were added and the mixture was allowed to last for 10 min. Then the nanoparticles were precipitated with a 2-propanol/methanol mixture (1:1−1:2), separated by centrifugation, and redissolved in hexane.

**Optical Characterization.** UV−vis absorption spectra were recorded with a Perkin-Elmer $\lambda$-2 and a Varian Cary 500 spectrometer. Luminescence measurements were performed with an Endinburgh Instruments FS920 fluorescence spectrometer with a slit size corresponding to a spectral resolution of 1 nm in excitation and 2 nm in emission. Photoluminescence quantum yields (PLQYs) were determined relatively to coumarin 2 dissolved in ethanol (PLQY of the coumarin 2 in ethanol: 93%).[22]

**X-ray Powder Diffraction (XRD).** XRD patterns were measured with a Bruker D8 Discover.

**Transmission Electron Microscopy (TEM).** TEM pictures and energy-dispersive X-ray (EDX) spectra were recorded with a JEOL 2200 FS electron microscope.

**Size Determination.** Size determination for nanoparticles with a diameter above 2 nm was performed by direct analysis of TEM images. Because of the low contrast for nanoparticles with diameters below 2 nm, an indirect approach was used: to estimate the size of these CdSe nanoparticles, the diameters of the corresponding core−shell structures were measured and the core diameters were calculated from the composition of the core−shell particles obtained via EDX.

## Hazards

When low-boiling solvents were injected, the temperature drop was caused by a superheating of the reaction mixture. Because of this, the quenching was performed in an open aperture under a nitrogen flow and *not* in a closed aperture under a nitrogen atmosphere. The dimensions of the reaction setup (e.g., the number of coolers attached) were well-chosen

(16) Kudera, S.; Zanella, M.; Giannini, C.; Rizzo, A.; Li, Y. Q.; Gigli, G.; Cingolani, R.; Ciccarella, G.; Spahl, W.; Parak, W. J.; Manna, L. *Adv. Mater.* **2007**, *19*, 548.
(17) Ouyang, J.; Zaman, M. B.; Yan, F. J.; Johnston, D.; Li, G.; Wu, X.; Leek, D.; Ratcliffe, C. I.; Ripmeester, J. A.; Yu, K. *J. Phys. Chem. C* **2008**, *112*, 13805.
(18) Talapin, D. V.; Rogach, A. L.; Haase, M.; Weller, H. *J. Phys. Chem. B* **2001**, *105*, 12278.
(19) Nielsen, A. *Kinetics of Precipitation*; Pergamon Press: Oxford, 1964; Vol. 18.
(20) Yu, W. W.; Qu, L. H.; Guo, W. Z.; Peng, X. G. *Chem. Mater.* **2003**, *15*, 2854.
(21) Li, J. J.; Wang, Y. A.; Guo, W. Z.; Keay, J. C.; Mishima, T. D.; Johnson, M. B.; Peng, X. G. *J. Am. Chem. Soc.* **2003**, *125*, 12567.
(22) Arbeloa, T. L.; Arbeloa, F. L.; Tapia, M. J.; Arbeloa, I. L. *J. Phys. Chem.* **1993**, *97*, 4704.

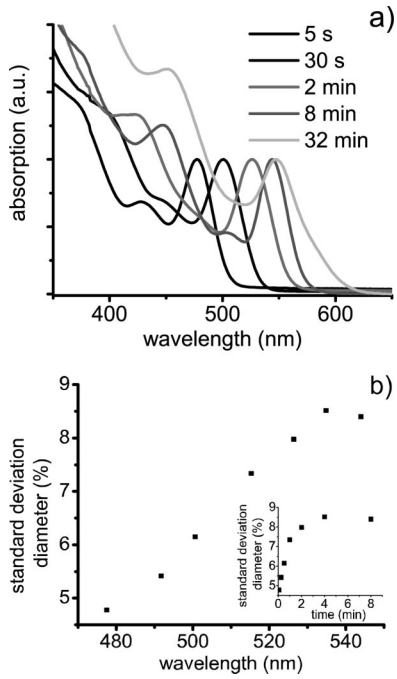


**Figure 1.** (a) Development of the absorption spectra with time of a CdSe QD synthesis according to the procedure described in the Experimental Section using stearic acid. Injection and growth temperature 245 and 230 °C, respectively, (b) development of the size distribution of the diameter vs $\lambda_{exc}$ (inset: development of the size dispersion vs $\lambda_{1s-1s}$ respectively the reaction time).

to avoid any reaction product to leave the reaction setup during the superheating.

## Results

**Overall Reaction Profile.** Figure 1a shows the development of the absorption spectra in a standard reaction where TOPSe is injected into a mixture containing cadmium stearate, stearic acid, and HDA. After 5 s, the first excitonic transition ($\lambda_{1s-1s}$) is observed at 474 nm, which shifts gradually to longer wavelengths with increasing reaction time. After 5 s the $\lambda_{1s-1s}$ absorption peak has a half-width at half-maximum (hwhm) of 15.9 nm or 85 meV. Assuming that this line width mainly reflects the dispersion of the particle size, the hwhm was used in combination with the sizing curve published by Yu et al.[20] to calculate the standard deviation of the quantum dot diameter distribution (size dispersion). With increasing reaction time, a regime of defocusing is observed with a gradual increase of the size dispersion from 4.8% (5 s) to about 8.5% after 4 min. After 4 min, the defocusing eventually stops and the size dispersion is slightly reduced to 8.4% after 8 min (Figure 1b). In the final stage of the reaction, a strong broadening of the size distribution was observed, probably due to Ostwald ripening. In summary, the sharpest size distribution is observed shortly after injection.

**Synthesis of Small CdSe Cores.** A reaction that yields narrow size distributions at short reaction times is well-suited for preparation of batches of small CdSe quantum dots, especially if it additionally offers control over the initial nanoparticle size. For this purpose, the effect of acid to amine ratio and the effect of the overall ligand concentration on the particles size after a short reaction time (5 s) was

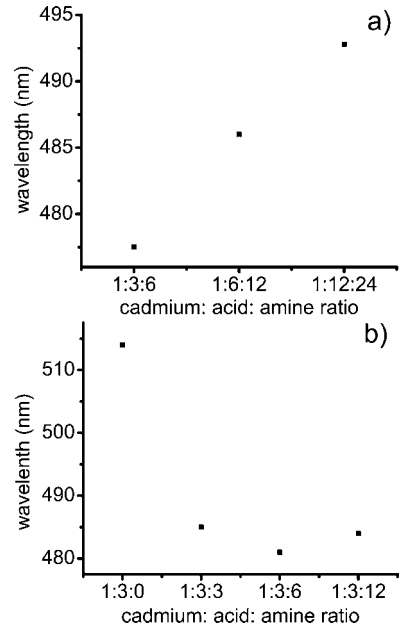


**Figure 2.** Dependence of the absorption wavelength observed after 5 s on (a) the overall ligand concentration and (b) the acid to amine ratio.

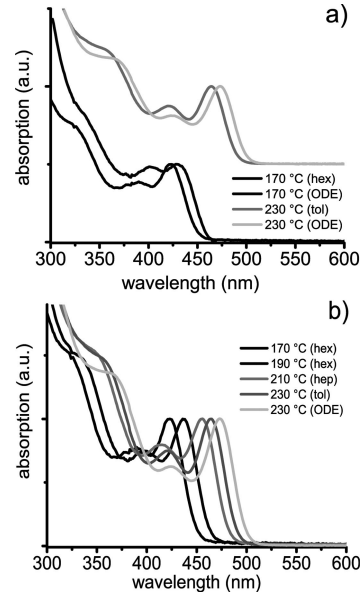


**Figure 3.** Absorption spectra for nanoparticle batches obtained for different injection temperatures and with different solvents for quenching after 5 s: hex, hexane; hep, heptanes; tol, toluene; ODE, 1-octadecene.

investigated (Figure 2). It turns out that the shortest $\lambda_{1s-1s}$ values are observed for a 1:2 acid to amine ratio and the lowest overall ligand concentration used. With the synthesis described above, size dispersions smaller than 5% are achieved after 5 s under these conditions, making this approach ideal for synthesizing small CdSe QDs.

To gain smaller particles, the injection temperature was reduced to slow down the reaction rate while the reaction time is kept constant (because of practical reasons, it was put aside to perform a reaction stop after shorter times than 5 s). In Figure 3a the absorption spectra of nanoparticle batches are shown, which were prepared at different injection temperatures and where the reaction was stopped by the injection of different solvents. Injecting a high-boiling solvent (ODE) leads in general to larger particles with broader size

**Table 1. Peak Positions of the First Transition in Absorption and Average Diameters for Nanoparticle Batches Obtained for Different Injection Temperatures with Different Solvents for Quenching after 5 s (in Brackets, Values for Second Reproduced Sample)[a]**

| sample name | injection temperature | quenching solvent | wavelength | diameter |
|---|---|---|---|---|
| 230ODE | 230 °C | ODE | 473 nm (471 nm) | 2.2 nm |
| 230tol | 230 °C | toluene | 462 nm (464 nm) | |
| 210hep | 210 °C | heptane | 456 nm (455 nm) | 1.9 nm |
| 190hex | 190 °C | hexane | 442 nm (437 nm) | 1.8 nm |
| 170hex | 170 °C | hexane | 423 nm (430 nm) | 1.6 nm |

[a] Sample notations: e.g., 230ODE, 230 °C injection temperature; reaction stopped by injection of ODE. hep, heptane; hex, hexane; tol, toluene. If indicated with cs, corresponding core−shell nanoparticles.

dispersion than low-boiling solvents like hexane and toluene. Especially for injection temperatures of 170 °C, the first electronic transition is significantly less pronounced when stopping the reaction by an injection of ODE as compared to an injection of hexane (the temperature drop by injection of a high-boiling solvent depends on the thermal energy of the high-boiling solvent and the heat capacity while the temperature drop caused by the injection of a low-boiling solvent depends on the boiling point of the resulting solvent mixture). This indicates that the reactivity of the precursors is still high enough to promote significant growth at low temperatures.

In Table 1 $\lambda_{1s-1s}$ of the samples obtained by stopping the reactions at different injection temperatures with given solvents are summarized. Its value varies between 423 and 473 nm (Figure 3b). The standard deviation on the wavelength of the first transition for different batches prepared under similar conditions is as small as 1−4 nm. Thus, the method is well-suited for the synthesis of very small CdSe QDs with a predefined size.

**Coating of Extremely Small Nanoparticles with Zinc Sulfide.** In Figure 4a the development of the absorption spectra during the coating procedure described above for 2.2 nm nanoparticles (sample 230 ODE) is shown. After addition of the nanoparticles to the reaction mixture, $\lambda_{1s-1s}$ drops from 473 to 465 nm during the heating to 90 °C. A similar behavior, albeit with a less pronounced initial shift of $\lambda_{1s-1s}$ to shorter wavelengths, is observed with smaller cores (cf. Figure 4b). After the growth temperature is reached, a progressive shift with time of $\lambda_{1s-1s}$ to longer wavelengths is observed for all core sizes. In the first 30 min the shift is significantly stronger for smaller sizes. As summarized in Tables 1 and 2, this results in a total red shift of $\lambda_{1s-1s}$ at the end of the coating procedure increasing from 6 nm for the largest QDs ($\lambda_{1s-1s}$: 473 nm, sample 230ODE) to 28 nm for the smallest QDs ($\lambda_{1s-1s}$: 423 nm, sample 170hex) (see also Table S1, Supporting Information).

Figure 5 shows TEM images of core nanoparticles (a,b) and of core−shell nanoparticles (c,d). As expected, the core−shell nanoparticles are larger than the simple core nanoparticles. Unfortunately, it becomes difficult to receive reliable values for the sizes of the core particles with TEM because of the low contrast for diameters below 2 nm. Therefore, only the diameters of the core−shell structures were measured and the shell thicknesses and the core diameters were calculated from the composition of the core−shell particles obtained via EDX (see Table S3, Supporting Information). Table 2 provides the measured diameters of core/shell particles together with the calculated core diameters and shell thicknesses. Using either the Cd:Zn ratio or the Se:S ratio leads to comparable core diameters that agree with those observed in the TEM pictures (sample 230ODE). The calculated shell thicknesses are in the range of 0.25−0.4 nm, i.e., about one ZnS monolayer (lattice spacing in the 111 direction ∼0.31 nm).

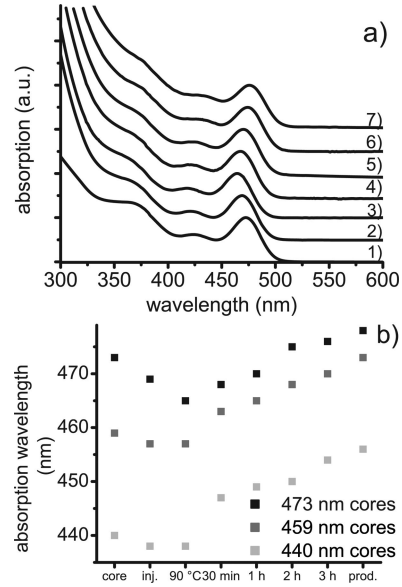


**Figure 4.** Development of the absorption spectra during the coating procedure: (1) stock solution; (2) after injection in the coating mixture; (3) after reaching the coating temperature; (4), (5), (6), and (7) after 30 min, 1 h, 2 h, and 3 h at the coating temperature, respectively. (a) Development absorption spectra during coating of sample 230ODE and (b) comparison of the development during the coating of different CdSe nanoparticles.

**Optical Properties.** The absorption and luminescence spectra of the core and core−shell nanoparticles are shown in Figure 6. With simple core nanoparticles, increasing trap emission is observed with decreasing particle size (Figure 6a). The photoluminescence quantum yield (PLQY) of the band gap emission drops from about 6% for 2.2 nm particles ($\lambda_{1s-1s}$: 473 nm, sample 230ODE) to below 1% for 1.6 nm particles ($\lambda_{1s-1s}$: 423 nm; sample 170hex; see Table S2, Supporting Information). The emission spectra of the corresponding core−shell nanoparticles show nearly no trap emission and the PLQYs of the band gap emission reach 40−50%, a value comparable to other results reported for CdSe/ZnS QDs (Figure 6b) (Figure 7).[12] This indicates a sufficient decoupling of the electronic wave functions of the exciton from the surface. As expected, the Stokes shifts increases both for core and core−shell materials with decreasing core size.[23]

**Crystal Structure.** For identification of the crystal structure, XRDs were taken from samples of particles with a diameter of about 2.2 nm ($\lambda_{1s-1s}$: 473 nm; sample 230ODE) and 3 nm ($\lambda_{1s-1s}$: 547 nm), and of 2.7 nm core−shell ($\lambda_{1s-1s}$: 476 nm; sample cs230ODE; Figure 7). At diameter of 2.2 nm it is impossible to distinguish between the possible wurzite and zinc blende structures (Figure 7a). For the 3 nm particles, the zinc blende modification can be clearly identi-

(23) Kuno, M.; Lee, J. K.; Dabbousi, B. O.; Mikulec, F. V.; Bawendi, M. G. *J. Chem. Phys.* **1997**, *106*, 9869.

**Table 2. Diameters of CdSe Core, CdSe/ZnS Core−Shell Nanoparticles, and Shell Thickness Calculated from EDX Data[a]**

| samples core/core−shell nanoparticles | average diameter core nanoparticles | average diameter core/shell nanoparticles | shell thickness |
|---|---|---|---|
| 230ODE/cs230ODE | 2.22 nm ± 0.06 nm<br>2.28 nm ± 0.06 nm<br>(2.16 nm ± 0.04 nm) | 2.74 nm ± 0.08 nm | 0.26 nm ± 0.03 nm<br>0.23 nm ± 0.03 nm<br>(0.28 nm ± 0.05 nm) |
| 210hep/cs210hep | 1.86 nm ± 0.13 nm<br>1.97 nm ± 0.07 nm | 2.45 nm ± 0.05 nm | 0.30 nm ± 0.07nm<br>0.24 nm ± 0.04 nm |
| 190hex/cs190hex | 1.51 nm ± 0.05 nm<br>1.86 nm ± 0.06 nm | 2.33 nm ± 0.04 nm | 0.41 nm ± 0.03 nm<br>0.24 nm ± 0.03 nm |
| 170hex/cs170hex | 1.54 nm ± 0.05 nm<br>1.63 nm ± 0.09 nm | 2.34 nm ± 0.08 nm | 0.40 nm ± 0.03 nm<br>0.36 nm ± 0.03 nm |

[a] Upper value, calculated on the cation composition; lower value, calculated on the anion composition; in brackets, value measured from TEM images.

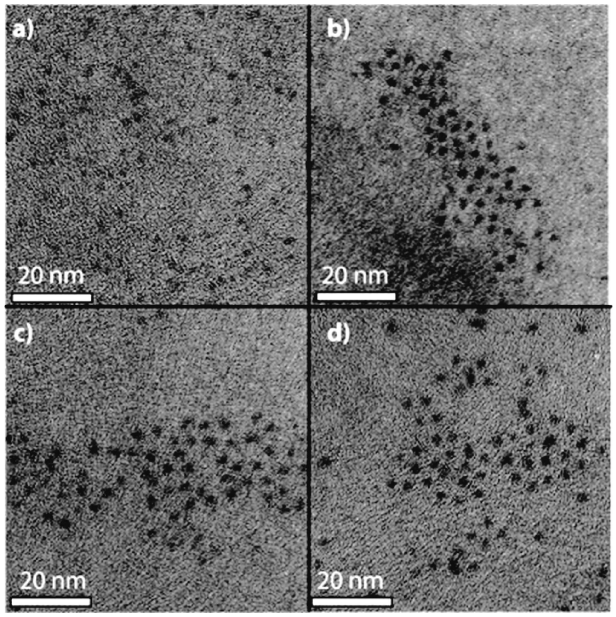


**Figure 5.** TEM images of CdSe QDs: (a) 170hex and (b) 230ODE and CdSe/ZnS core−shell nanoparticles: (c) cs170hex and (d) cs230ODE.

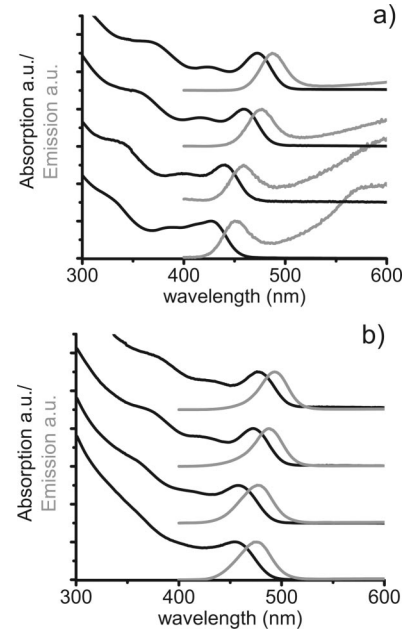


**Figure 6.** Absorption and emission spectra of (a) core and (b) core−shell nanoparticles. (a) Samples from bottom to the top: 170hex, 190hex, 210hep, and 230ODE; (b) samples from bottom to the top: cs170hex, cs190hex, cs210hep, and cs230ODE.

fied (Figure 7a). This result is in agreement with the literature.[7]

The XRD of the core−shell particles is similar to that of noncoated particles, although the diameter of the particles increases from 2.2 to 2.7 nm (Figure 7b).

## Discussion

**Synthesis Strategy Based on High Oversaturation.** In general, CdSe synthesis schemes designed for the formation of monodisperse nanoparticles rely on size distribution focusing. This concept makes use of the change of the growth speed of colloidal particles dependent on their size compared to the critical radius: for particle sizes close to the critical radius, the growth speed of the particles increases with increasing size, while for larger particle sizes the growth speed decreases (Figure 9). Although highly successful, a disadvantage of this approach is that relatively broad size dispersions are obtained after short reaction times.[24] Hence, a focusing-based synthesis is not the best choice for synthesizing sub-2-nm CdSe QDs of low size dispersion.

(24) Peng, X. G.; Wickham, J.; Alivisatos, A. P. *J. Am. Chem. Soc.* **1998**, *120*, 5343.

Within the concepts of classical nucleation theory,[18,19] a synthesis capable of providing particles of this size needs a sufficiently small critical radius $r_{crit}$ and a high nucleation rate $J$. The first determines the smallest size reachable by the synthesis and the second warrants a high yield of small particles at short reaction times. According to classical nucleation theory, both quantities can be estimated as follows:

$$r_{crit} = \frac{2\sigma V_m}{RT \ln S} \quad (1)$$

$$J \propto \exp\left(-\frac{16\pi\sigma^3 V_m^{\,2}}{3(RT)^3(\ln S)^2}\right) \quad (2)$$

Here, $\sigma$ is the interfacial tension, $V_m$ is the molar volume of the solid material, $R$ is the gas constant, $T$ is the temperature, and $S$ is the saturation ratio $c/s$, where $c$ is the concentration and $s$ the solubility of the precipitant.

The equations show that both parameters can be optimized in the direction of a small critical radius and a high nucleation

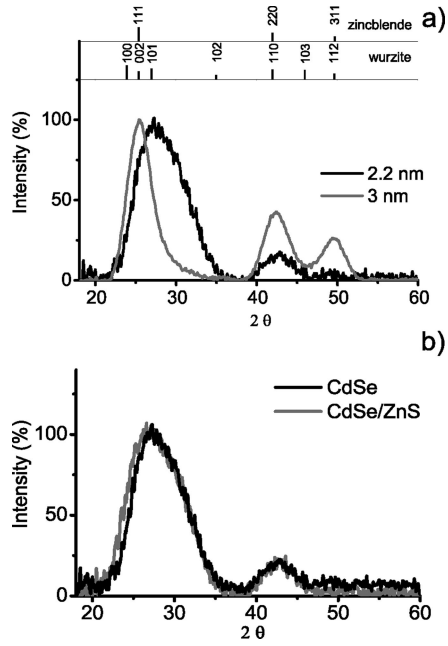


**Figure 7.** XRD patterns of samples (a) for CdSe QDs (2.2 and 3 nm in diameter, bulk pattern for zinc blende and wurzite modification indicated) and (b) XRD patterns of CdSe QDs (2.2 nm in diameter) and corresponding CdSe/ZnS QDs (2.7 nm in diameter).

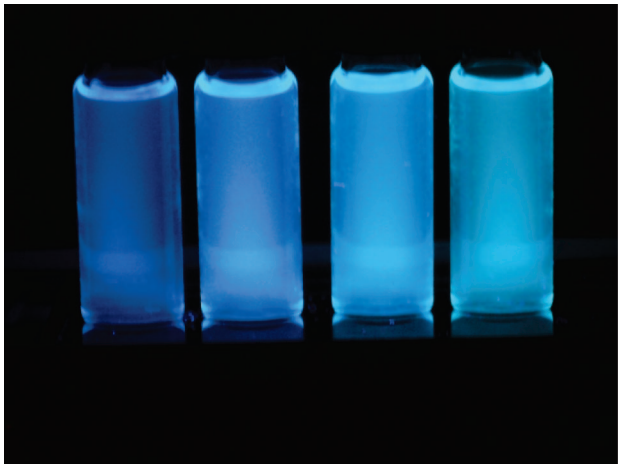

**Figure 8.** Image of solutions of CdSe/ZnS QDs under UV irradiation with emission wavelengths from left to right: 475, 478, 488, and 494 nm.

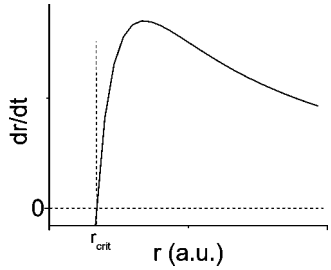


**Figure 9.** Typical dependence of the growth speed of a particle depending on its size in an oversaturated regime.[29]

rate by increasing the saturation ratio. This can be achieved by a reduction of the solubility of the precipitant in the reaction mixture. Therefore, typical cadmium carboxylate (respectively, cadmium phosphonate) and alkyl phosphine chalcogenide-based cadmium chalcogenide synthesis[25,26] were adopted and the ligand (free acid and alkyl amine concentrations) composition was modified considering the following assumptions:

1 The solubility of metal chalcogenides decrease in aqueous media with increasing pH value. Assuming that this concept can be transferred to lipophilic solvent mixtures, we can expect that alkyl amines act as a "basic agent", reducing the solubility of the precipitant.

2 The ligands used in the typical hot-injection mixtures are also solvents of the particular materials. Therefore, the ligand concentration should be reduced as much as possible, without losing the solubility of the metal precursor (here CdO).

In accordance with these assumptions, the smallest particles (respectively the shortest $\lambda_{1s-1s}$) are observed for an acid:amine ratio of 1:2 and the smallest overall ligand concentration (Figure 2).

The development of the size distribution of this reaction (Figure 1b) shows a different behavior than reactions designed for size distribution focusing, featuring mainly a defocusing of the initially narrow size distribution. A tentative explanation for the sharp size distributions at an early stage of the reaction can be given as follows. In the beginning of the reaction, first nuclei are formed. These nuclei consume precipitant out of the reaction mixture and the concentration of the precipitant drops. Taking eq 1 into account, a drop of the concentration of the precipitant leads to an increase of the critical radius. Since the radii of the particles present at this stage of the reaction are still close to the initial critical radius, we assume that the critical radius reaches a value larger than the radius of the majority of the particles present. This leads to the dissolution of the smaller particles and an initial focusing of the size distribution takes place.

A further advantage of the synthesis described here is the high reproducibility of the size and hence the optical properties of the obtained nanoparticles (Table 1). This can be addressed to the relatively short and, by this, highly reproducible temperature program which only depends on the heat capacity of the reaction system and will remain the same as long as the same setup is used.

**Comparison with Magic-Sized Clusters.** Recently, research results have been published, where magic-sized CdSe nanoparticles (clusters) were used as fluorescence dyes or as cores for fluorescent core−shell nanoparticles.[16,27] These clusters show $\lambda_{1s-1s}$ between ca. 330 and 513 nm and main emission bands up to wavelengths of 516 nm.[16,17] Therefore, cluster synthesis represents an approach that is complementary to the method described here for CDSe QDs in a size range of 1.6−2.2 nm in diameter.[14−16,25,26] It was assumed that clusters are particles with a radius below the critical radius (embryos),[16] while we expect that the prefocused QDs reported here (all with $\lambda_{1s-1s}$ below the largest reported cluster)[17] are formed above the critical radius. The comparison of the results reported indicates that size dispersions obtained due to embryo growth are driven mainly by magic sizes (material properties) while size dispersions obtained

(25) Qu, L. H.; Peng, Z. A.; Peng, X. G. *Nano Lett.* **2001**, *1*, 333.
(26) Yu, W. W.; Wang, Y. A.; Peng, X. G. *Chem. Mater.* **2003**, *15*, 4300.
(27) Kucur, E.; Ziegler, J.; Nann, T. *Small* **2008**, *4*, 883.

due to nuclei growth are driven by the reaction conditions. From a practical point of view, embryo growth bares the advantage of extremely sharp main size distributions, while nuclei growth offers the possibility of free sizing and enables elimination of undesired sizes by mechanisms like prefocusing or focusing. [14−16,27]

**Core−Shell Nanoparticles.** After coating of the core nanoparticles, a shift to longer wavelengths of the first transition in the absorption and of the peak wavelength of the emission signal is observed. This effect is stronger for smaller particles, which is in agreement with the literature,[12,28] yet it is the net result of two underlying trends. First, the first absorption and the emission peak show a weaker blue shift for smaller nanoparticles after their addition to the coating mixture and during heating up to the coating temperature (Figure 4). Second, smaller particles exhibit a stronger red shift of these features with time after the coating temperature is reached. The increasing red shift of the first absorption and emission maximum during the coating with decreasing size of the CdSe cores can be explained by a stronger leakage of the excitonic wave functions into the shell with decreasing size of the nanoparticle core.[12] The origin of the initial blue shift is less clear. It may indicate that the QDs slightly dissolve after addition to the reaction mixture. Taking into account that the confinement increases at a greater rate with decreasing size, the decreasing shift of the absorption and emission features would imply that the smallest particles dissolve less. A practical consequence of this observation is that the region of extreme confinement or very small diameters is not favorable for an effective adjustment of the emission to short wavelengths: the smallest CdSe nanocrystals suffer from a strongly increasing Stokes shift (Table S2),[23] and a stronger red shift of the first transition after coating (Figure 5, Table S1, and Table S2). On the other hand, it should still be possible to reach even shorter emission wavelengths by this procedure by reduction of the thickness of the coating.[14]

## Conclusions

In this work, we present a strategy for the synthesis of highly monodisperse batches of extremely small cadmium selenide nanoparticles with sizes down to the cluster range. These particles were used as cores for cadmium selenide/zinc sulfide QDs which are brightly luminescent and show emission wavelengths as short as 475 nm. Zinc sulfide coating could be achieved, using a procedure based on zinc carboxylates and sulfur dissolved in octadecene and, by this, without the use of highly reactive (dangerous) reagents like diethyl zinc. Since the longest wavelength for emission of cadmium sulfide/zinc sulfide QDs reported is 480 nm, this approach provides a pathway to cover the visible range with II−VI type-I core−shell nanoparticles down to the UV. Furthermore, the mentioned strategy for the preparation of small particles is not necessarily specific to CdSe and should also apply to other systems like other known II−VI or IV−VI semiconductor nanoparticle syntheses.

**Acknowledgment.** R.Č. and Z.H. acknowledge BelSPO (IAP VI.10, photonics@be) and the FWO-Vlaanderen for funding this research (G.0.144.08).

**Supporting Information Available:** Additional data about the materials prepared. This material is available free of charge via the Internet at http://pubs.acs.org.

CM900248B

(28) Eychmuller, A.; Mews, A.; Weller, H. *Chem. Phys. Lett.* **1993**, *208*, 59.
(29) Sugimoto, T. *Adv. Colloid Interface Sci.* **1987**, *28*, 65.